Modelling the dynamics of infection, waning of immunity and re-infection with the Omicron variant of SARS-CoV-2 in Aotearoa New Zealand

Giorgia Vattiatio[1,2], Audrey Lustig[3], Oliver Maclaren[4], Michael J. Plank[2]

1. Department of Physics, University of Auckland, Auckland, New Zealand.
2. School of Mathematics and Statistics, University of Canterbury, Christchurch, New Zealand.
3. Manaaki Whenua, Lincoln, New Zealand.
4. Department of Engineering Science, University of Auckland, Auckland, New Zealand.

Submitted for internal peer review: 13 May 2022

Revised: 31 May 2022

Executive summary

1. Waning of infection-derived immunity means people become increasingly susceptible to being re-infected with SARS-CoV-2 over time. This waning creates the possibility of subsequent waves of infection, even after substantial population exposure, driven largely by re-infections.
2. We investigated a model that included the effects of waning of vaccine-derived and infection-derived immunity under scenarios representing different levels of behavioural change relative to the first Omicron wave, and varying assumptions about the durability of infection-derived immunity, which is uncertain.
3. In all scenarios investigated, a second wave of infections occurred in the second half of 2022. The timing of the peak of the second wave depended primarily on the speed at which immunity wanes following infection and was typically between August and November 2022 in the scenarios tested.
4. The peak number of daily cases in the second wave was smaller than in the first wave.
5. The peak hospital occupancy in the second wave was also generally smaller than in the first wave, but this was sensitive to the number of infections occurring in older age groups. A scenario with increased contact rates in older groups led to peak hospital occupancy higher than in the first wave.
6. Scenarios with relatively high transmission rates (whether a result of relaxation of public health measures or voluntary behaviour change) did not necessarily lead to higher peaks. However, they generally resulted in more cumulative cases and sustained demand on healthcare systems (>250 hospital beds occupied throughout the winter period).
7. The estimated health burden of Covid-19 in the medium term is sensitive to the strength and durability of infection-derived and hybrid immunity against severe illness, which are uncertain.

Background

We have previously modelled the first wave of the Omicron variant of SARS-CoV-2 in New Zealand using an age-structured model (1). This model included the effects of age-specific vaccination rates, different vaccine effectiveness against different clinical endpoints, and waning of vaccine-derived immunity. However, the model did not include the effects of waning of infection-derived immunity, meaning that people could not be infected with the virus for a second time. This assumption meant that, after the first wave, the epidemic died out in the model as the number of susceptible people became too low to sustain transmission.

In reality, infection-derived immunity against SARS-CoV-2 likely wanes over time, meaning it is possible for people to be infected more than once. Mathematically, this means that transmission of the virus does not die out and instead gives rise to a stable equilibrium state in which a steady fraction of the population is infected with the virus per day, balancing loss of immunity through waning. The number of new infections typically tends towards the equilibrium state via a sequence of progressively smaller waves (2). In reality, this pattern is affected by factors such as changing behaviour, age distribution of new infections, antigenic evolution, and seasonality. However, attraction towards the equilibrium is a strong driving force in the epidemic dynamics.

Here, we extend our previous model to include waning of infection-derived immunity and consequent re-infection. We investigate scenarios with different levels of contact rates in different age groups and how these affect the size and timing of a second wave. We also conduct a sensitivity analysis to the strength and rate of waning of infection-derived immunity, as there is currently significant uncertainty around these. These results may be helpful for planning healthcare capacity over the winter months and to inform measures to mitigate the ongoing health burden of Covid-19.

Model scenarios

We considered four scenarios for changes in contact rates following the peak in reported cases for the first Omicron wave, which occurred around 5 March 2022. These represent relaxation of public health measures as well as voluntary changes in precautionary behaviour. The exact magnitude of these was unknown in advance, so we investigated the effects of contact rates increasing by differing amounts during March and April 2022 (Table 1). During the first wave, reported cases of Covid-19 have been relatively concentrated in younger age groups. This may be partly due to heightened levels of precautionary behaviour among older age groups, which might be expected to reduce over time due to fatigue with precautions or reduction in perceived risk. We therefore also investigated a scenario in which there is an additional increase in contact rates in older age groups (Table 1), representing a return towards pre-pandemic mixing patterns between age groups (3).

In addition to changes in contact rates, the strength and durability of infection-derived immunity and hybrid immunity following infection with Omicron are highly uncertain. We investigated three models with different speeds of waning of infection-derived immunity, which we refer to as the baseline, fast waning and slow waning scenario (see Figure 1). We assumed in all cases that immunity to severe disease and death is higher and longer-lasting than immunity to infection. Our assumptions are broadly within the range of values estimated by the model of (4-6), which is based on the relationship between neutralising antibody titres, which decline over time, and immunity against different clinical endpoints. Our assumptions on immunity to severe disease and death correspond to somewhat flatter curves than those of the above model, with immunity maintained at a higher level over more extended time frames (though see Supplementary Figure S5 for a sensitivity analysis).

Scenario	Reproduction number	Age-specific contact rates
A	13% increase over 10 days from 10 March	No change
B	40% increase over 30 days from 10 March	No change
C.1	67% increase over 50 days from 10 March	No change
C.2	67% increase over 50 days from 10 March	Higher contacts with older age groups from 1 July

Table 1. Summary of assumptions in the four main scenarios about overall transmission rate, measured by the reproduction number, and age-specific contact patterns in the four main model scenarios. Changes in reproduction number are reported as relative changes to the reproduction number excluding immunity R_{EI}, which was assumed to be $R_{EI} = 2.5$ in the period prior to 10 March 2022. The value of R_{EI} was increased linearly over a specified period of time starting on 10 March. This date was chosen as it followed the peak in reported cases, modelling a component of reactive voluntary behaviour change, and gave a reasonable match with the observed decline in cases following the peak, which was slower than would be expected with a fixed value of R_{EI}. The switch from the Red to the Orange setting of the Covid-19 Protection Framework on 13 April 2022 was not explicitly linked to the timing of these scenarios, but likely contributed to the increase in R_{EI}, particularly in scenario C.

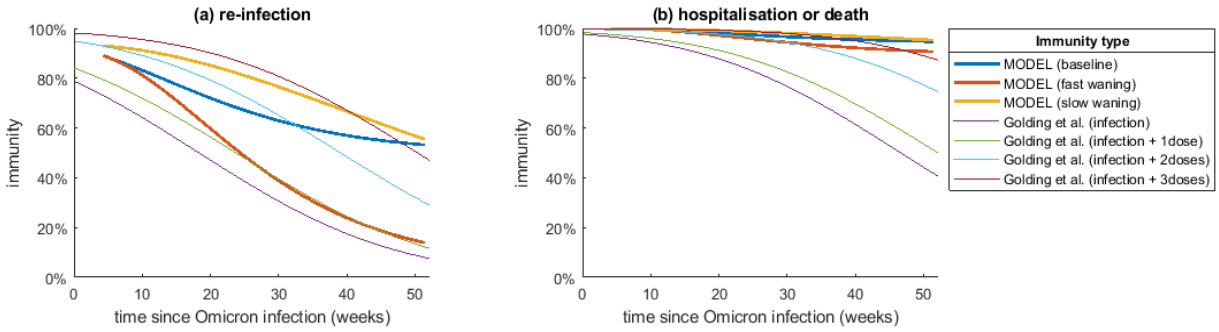

Figure 1. Three model scenarios for average post-infection immunity against: (a) re-infection and (b) hospitalisation or death, over time since previous infection, for people who have had at least one dose of the vaccine. People who are unvaccinated start with a lower level of immunity following their first infection. For comparison, we show the immunity estimates of (6) based on the model of (4, 5), following infection with Omicron (note as a simplifying assumption our model assumes the same level of infection-derived immunity for vaccinated people regardless of the number of doses received).

Results

Results for the four contact rate scenarios and three models of infection-derived immunity are shown in Figure 2 and Table 2. These results were produced in mid-April 2022. In all scenarios, a second wave of infections occurred in 2022, driven by a mixture of people not infected in the first wave and re-infection of people whose immunity has waned (Supplementary Figure S4). The peak number of new daily cases in the second wave in the model was significantly smaller than in the first wave. The peak hospital occupancy was also generally smaller, with the exception of the scenarios with increased contact rates among older groups. In these scenarios, peak hospitalisations and total deaths exceeded the first wave. This was due to a shift in the age distribution of cases (Figure 3): although the overall distribution was still dominated by under 35s, relatively small increases in the proportion of cases in over 60s had a major impact on hospitalisations and deaths due to the steep age gradient in risk. This shows that the overall health burden is highly sensitive to the number of infections in high-risk groups. It should be remembered that Māori and Pacific people are known to have higher risk of severe illness after controlling for age (7).

In the scenario with the largest increase in contact rates (scenario C), there was a small secondary wave in May/June 2022 driven by the increased ability of the virus to find new hosts that had not been previously infected. This had the effect of reducing the size of the subsequent wave that occurred later in the year, as there was more immunity and fewer naive hosts at that time. However, the cumulative numbers of infections, hospitalisations and deaths were still larger in scenario C than in scenarios A and B (Table 2).

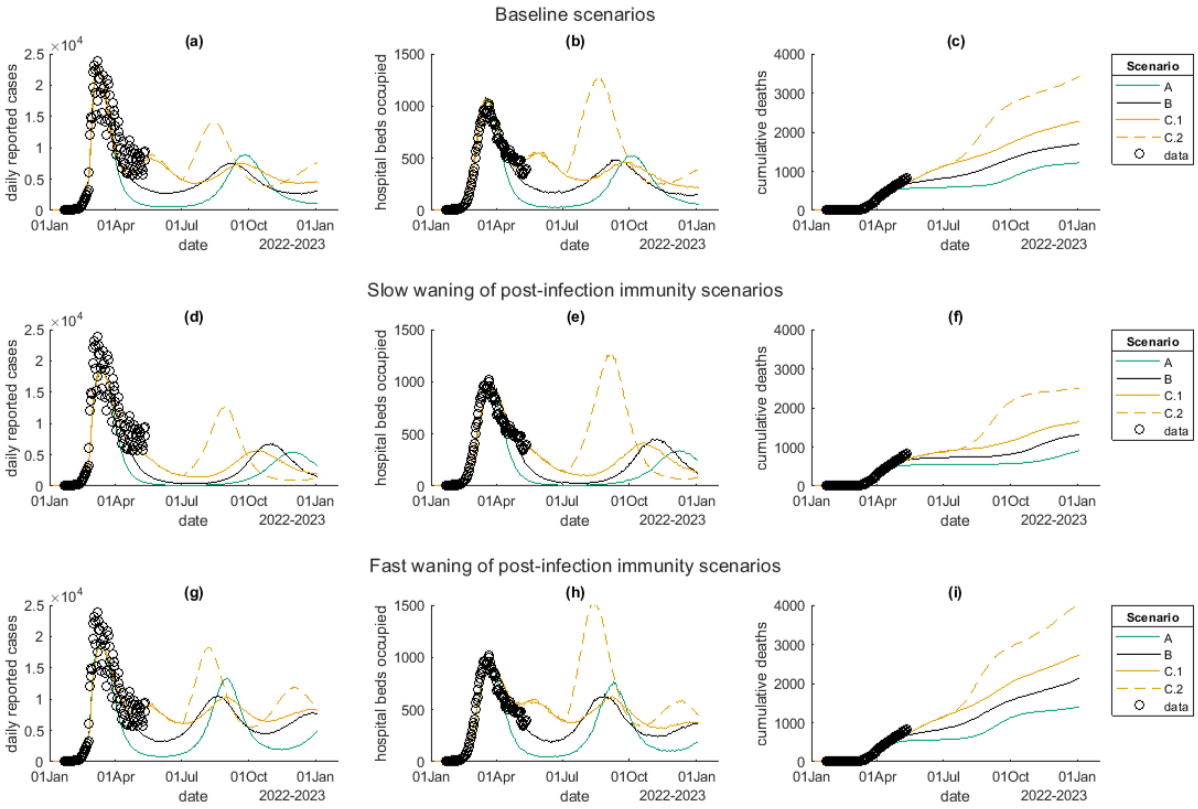

Figure 2. Model results for daily reported cases (a,d,g), number of hospital beds occupied (b,e,h), and cumulative deaths (c,f,i) for the four scenarios A (green), B (black), C.1 (solid yellow) and C.2 (dashed yellow), under the baseline model for post-infection immunity (a-c), slow waning of post-infection immunity (d-f), and fast waning of post-infection immunity (g-i). Black circles show data up to 12 May 2022.

Scenario		Infections	Cases	Hosp	Deaths	CAR	Re-infections
Baseline	A	3,831,000	1,452,000	21,500	1,210	38%	20%
	B	4,905,000	1,872,000	28,200	1,700	38%	27%
	C.1	6,033,000	2,318,000	35,200	2,290	38%	34%
	C.2	6,932,000	2,690,000	46,700	3,430	39%	37%
Slow waning of post-infection immunity	A	2,965,000	1,113,000	16,400	910	38%	12%
	B	3,693,000	1,412,000	22,300	1,320	38%	15%
	C.1	4,216,000	1,617,000	26,400	1,640	38%	18%
	C.2	4,697,000	1,834,000	36,300	2,500	39%	17%
Fast waning of post-infection immunity	A	4,505,000	1,703,000	24,100	1,400	38%	28%
	B	6,124,000	2,341,000	33,200	2,140	38%	37%
	C.1	7,280,000	2,797,000	40,000	2,740	38%	43%
	C.2	8,326,000	3,254,000	52,900	4,060	39%	46%

Table 2. Total number of infections, cases, hospitalisations, and deaths, case ascertainment rate (CAR) calculated as the ratio of total number of cases to total infections, and proportion of total cases that are reinfections in the model, over the simulated time period (365 days starting on 5 January 2022) for each of the scenarios described in Table 1. Note that the observed number of re-infections would appear lower than model results suggest if the previous infection was not confirmed in some fraction of these.

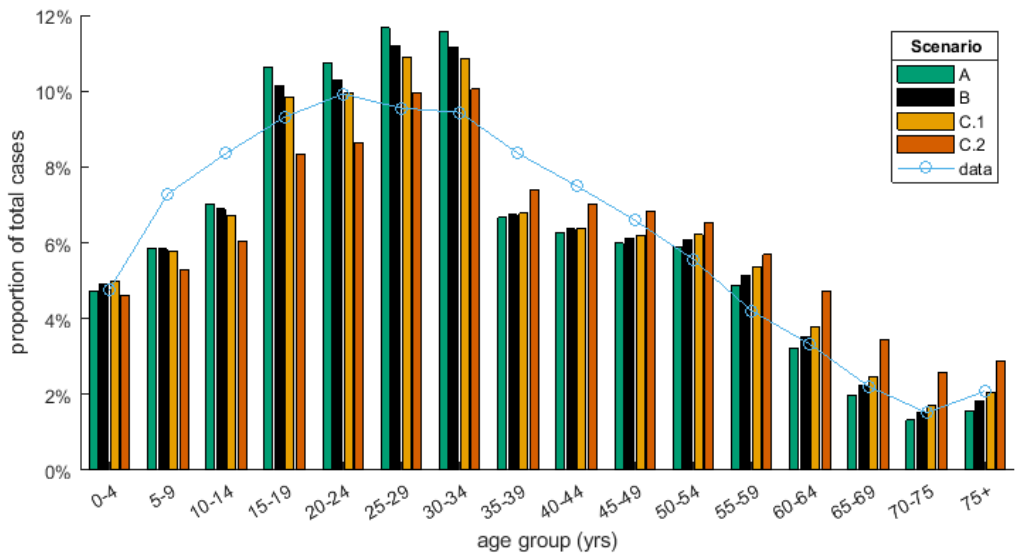

Figure 3. Age distribution of cases in model scenarios A, B, C.1 and C.2 (coloured bars), alongside data on the age distribution of reported cases from 25 January to 10 May 2022 (blue curve).

The size and timing of the second wave in the model was sensitive to assumptions about the speed of waning of immunity from prior infection, with faster waning generally associated with earlier waves, slightly higher peaks and significantly larger numbers of cumulative infections, hospitalisations and deaths.

The model has been calibrated against data on reported cases, hospitalisations and deaths up to mid-April 2022. However, these data sources have biases that may affect model behaviour. Reported cases represent an unknown fraction of total infections, and this means that the amount of infection-derived immunity that has built up in the population through the first wave is uncertain. Hospitalisation data includes a mixture of people who are being treated for Covid-19 and people who are being treated for other conditions but test positive before or during their stay in hospital. Reported deaths include everyone who has died within 28 days of a positive Covid-19 test result. This may include some incidental deaths, particularly in younger age groups. Model outputs should be interpreted with caution in the context of these known data limitations.

The scenarios shown in Figure 2 attempt to capture some of the uncertainty in two key variables driving epidemic dynamics: (1) changing contact rates as a result of relaxing public health measures and voluntary behaviour change; and (2) the strength and durability of infection-derived immunity. The model parameters used in these scenarios cover a reasonable range of outcomes based on previous estimates of changes in contact rates and estimates of the dynamics of waning immunity from different sources against different clinical endpoints (4, 5, 8). However, it is possible that outcomes will fall outside these ranges. In particular, there is limited population-level data at present on time-varying immunity (with or without vaccination) against re-infection with the same Omicron variant, so these estimates are uncertain. In addition, the health impacts of any

second wave will depend on the strength and durability of infection-derived immunity to severe illness.

Uncertainty concerning model scenarios is compounded by the emergence of new sub-variants of Omicron with different transmissibility and immune escape characteristics. For example, New Zealand's first Omicron wave was dominated by BA.2 with a significant minority of BA.1 infection (9). If a new subvariant becomes dominant, such as BA.4 or BA.5, which can more easily re-infect people previously infected with BA.1 or BA.2 (10), this could cause a second wave to happen earlier than it would otherwise. This wave's health impact would largely depend on the degree to which prior infection with BA.1 or BA.2 protects against severe illness with the new sub-variant. The scenarios presented here do not attempt to capture the effects of a new variant of concern with a substantial increase in transmissibility, immune escape and/or virulence. However, this model framework is being used in a separate piece of work to investigate the potential impact of hypothetical new variants with specific epidemiological characteristics.

The model ignores important sources of heterogeneity in the New Zealand population that could affect rates of transmission and health burden over time. Model results show the national picture but this is likely to be unevenly distributed across the population. Communities with low vaccination rates, high comorbidity rates, poorly served by healthcare systems, or other risk factors are likely to be disproportionately affected. Māori and Pacific people in particular have experienced very high transmission rates during the first wave and are at higher risk of severe illness if infected with SARS-CoV-2 (7). Reinfections are likely to be clustered in particular communities at different times due to the persistence of particular transmission networks, which could lead, for example, to acute worker shortages in some workplaces or sectors. The model results for scenario C.2 show that the health impacts of a second wave will be highly sensitive to the number of infections occurring in older age groups. This will also apply to other high-risk groups, including Māori and Pacific people and people who are immunocompromised or have other comorbidities, although these factors were not explicitly included in the model.

Key model assumptions

Vaccine coverage in each five-year age group over time was based on Ministry of Health data on the number of first, second and third doses of the vaccine given each day up to 4 May 2022 (Supplementary Figure S1). Model assumptions around vaccine effectiveness and disease severity were as described in (1). We increased the assumed fatality rate for the over 75 year age group by a factor of 1.6 to achieve a better match with the observed case fatality rate in this group (3.1%).

The generation interval, in the absence of interventions, was assumed to have mean 3.3 days and standard deviation 1.3 days. We assumed that, at the beginning of the outbreak, 30% of symptomatic infections become confirmed cases, with an average of 4 days from symptom onset to positive test result. However, in late February, New

Zealand introduced widespread use of rapid antigen tests (RATs), following a large backlog of unprocessed RT-PCR tests. The switch to RATs as the main form of testing was associated with a jump in reported cases. As an approximate model of this, from 23 February onwards we increased the proportion of symptomatic infections that become confirmed cases to 50% and reduced the average time from symptom onset to positive test result to 1.5 days (the time from symptom onset to test result for 577,370 cases between 1 March and 30 April 2022 with onset date recorded was 1.9 ± 2.1 days). These parameters gave a reasonable empirical match with the change in trends in reported cases that occurred at this time, although other parameter combinations are also possible (see Supplementary Information for details).

Mixing within and between age groups is described in the model by an age-dependent contact matrix based on pre-pandemic survey data (3) and adjusted for the New Zealand population (11). To approximate the age distribution of reported cases during the first wave (Figure 3), we used an adjusted form of this pre-pandemic contact matrix with reduced contact rates for older groups relative to younger groups (see Supplementary Table S2). This adjustment may partly reflect heightened levels of precautionary behaviour in high-risk demographic groups. In the scenario with increased contact rates in older groups during the second wave, we used a contact matrix representing contact patterns intermediate between those of the first wave and those corresponding to the matrix used in (11) based on pre-pandemic estimates. This change in contract matrix was assumed to take effect on 1 July 2022, which led to a sudden start to the second wave in model results. This was a simplifying assumption and it is likely that, in reality, any change would take place more gradually and could occur earlier or later than assumed.

Following infection, individuals were assumed to remain completely immune to re-infection for a fixed period of 30 days. At the end of this period, immunity was assumed to decline over time (see Figure 1) based on estimates from (6). As a simplifying assumption, we assumed that infection-derived immunity is the same for individuals who have had one, two or three doses of the vaccine. However, unvaccinated people were assumed to start at a lower level of immunity following their first infection (see Supplementary Table S1), reflecting evidence that infection with Omicron elicits a substantially weaker antibody response in unvaccinated people compared to vaccinated people (10). Following recovery from a second or subsequent infection, all individuals' immunity were assumed to follow the curves shown in Figure 1 regardless of vaccination status. The risks of hospitalisation and death are age-dependent in the model (see Supplementary Table S3) but the relative reduction in risk due to immunity was assumed to be age-independent.

Immunity from infections that occurred prior to the start of the simulated time period (January 2022) was ignored. This assumption is not likely to have a large effect on model results given that, prior to the arrival of Omicron, New Zealand has had approximately 12,600 confirmed community cases of Covid-19, which is around 0.25% of the total population.

The effects of seasonality were not included in the model. Simulations were initialised with 500 seed infections introduced over a one-week time period starting on 5 January 2022. Key model outputs were not highly sensitive to seeding assumptions, which were chosen to give a reasonable match to the initial growth phase of the first wave. We also assumed an average of 50 daily infections arriving at the border. This prevented simulations from stochastically eliminating, but did not otherwise have a significant effect on model results.

Acknowledgements

The authors acknowledge the support of the New Zealand Ministry of Health, StatsNZ, and the Institute of Environmental Science and Research in supplying data in support of this work. The authors are grateful to Emily Harvey, Nick Golding, James McCaw, Dion O'Neale and Freya Shearer for discussions about modelling waning immunity, and to Samik Datta, Nigel French, Anja Mizdrak, Matt Parry, and the COVID-19 Modelling Government Steering Group for feedback on earlier versions of this report. Kannan Ridings helped with data management. This work was funded by the New Zealand Department of Prime Minister and Cabinet.

Supplementary information

We used an age-structured stochastic model for transmission of SARS-CoV-2. This builds on a model that has previously been used to describe New Zealand's Omicron outbreak, which includes the effects of two-dose and three-dose vaccine coverage in five-year age bands and waning of vaccine-induced immunity over time (1). Here, we generalised this model to include waning of infection-induced immunity, which means individuals can be re-infected multiple times.

Test-trace-isolate-quarantine model

We assumed that infected individuals become confirmed cases with probability p_{test}, and detection occurs with an exponentially distributed delay from symptom onset with mean $t_{onset \to isol}$. According to Ministry of Health data, the time from symptom onset to test result for the 577,370 cases between 1 March and 30 April 2022 with an onset date reported was 1.9 ± 2.1 days suggesting that an exponential distribution is a reasonable approximation. For a given overall effect of test-trace-isolate-quarantine measures on R_{eff}, model results were not highly sensitive to the shape of the assumed onset to detection distribution. We assumed that subclinical individuals are not triggered to get tested by symptoms, although they may be detected via contact tracing (see next paragraph).

In addition to symptom-triggered testing, we assumed that a proportion $p_{trace} = 0.25$ of contacts (whether clinical or subclinical) of a confirmed case are identified via contact tracing and quarantined with a mean of 3 days from confirmation of the index case. The relatively low value of $p_{trace} = 0.25$ reflects a system that primarily involves quarantine of household contacts as opposed to active case finding and contact tracing by public health units.

We use quarantine to refer to pre-symptomatic or asymptomatic individuals identified via contact tracing who have not yet returned a positive test result, and isolation to refer either to contacts who have developed symptoms or to confirmed cases. We assumed quarantine reduces transmission to c_{quar} and isolation reduces transmission to c_{isol}, relative to non-quarantined individuals.

We used two sets of parameters for p_{test}, $t_{onset \to isol}$ and c_{isol}, one for the period up to 22 February 2022 and one for the remainder of the simulation, to give a reasonable match to the change in reported case trends following the change from PCR testing to rapid antigen tests as the main form of testing (Supplementary Table S4).

Vaccine coverage and vaccine effectiveness

Time-varying vaccine coverage in five-year age bands was as per data on doses administered up to 4 May 2022, with the additional assumption that everyone who had received their first dose by 4 May receives their second dose ten weeks later (if under 15 years old) or five weeks later (if over 15 years old). Note that model vaccine coverage may be lower than official Ministry of Health statistics because we used the StatsNZ estimated resident population (ERP) as population denominators (see Supplementary

Table S4), rather than the health service utilisation (HSU) population, which is typically smaller. All vaccine doses were assumed to take effect 14 days after being received. We did not assume any additional future uptake of vaccine (other than conversion of first dose to second dose) as vaccination rates have levelled off and, at the time the modelling was carried out, there were no confirmed plans to offer a fourth dose.

Vaccine effectiveness of the Pfizer/BioNTech BNT162b2 vaccine was characterised by three model parameters: reduction in risk of infection (e_I), risk of hospitalisation (e_D), and risk of death (e_M). Effectiveness was assumed to wane with time, modelled via a series of susceptible compartments based on time since most recent dose (Supplementary Table S1, Supplementary Figures S2-S3) – see (1) for details of data sources.

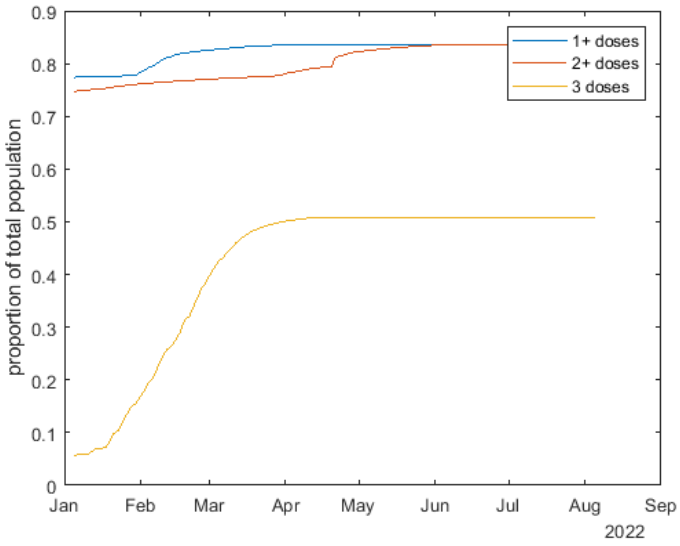

Supplementary Figure S1. Proportion of the total population who have received at least one dose, at least two doses, and three doses, plotted by date the immunity takes effect, which is assumed to be 14 days after the vaccine is received.

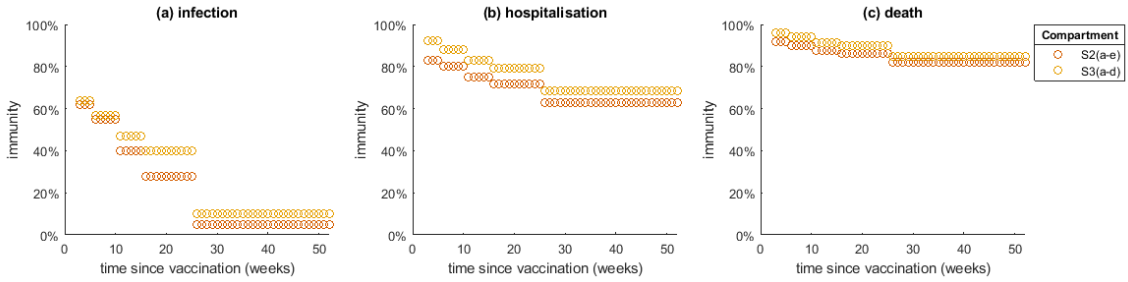

Supplementary Figure S2. Assumed vaccine-induced immunity against: (a) infection, (b) hospitalisation, and (c) death, over time since most recent dose for people with either two (red) or three (yellow) doses of the vaccine. People with only one dose of the vaccine are assumed to have no protection against infection, hospitalisation, or death until they receive their second dose.

Basic reproduction number and generation interval

We assumed the reproduction number excluding the effects of immunity (R_{EI}) was $R_{EI} = 2.5$ in the initial part of the first wave, and that R_{EI} then increased linearly over a specified period of time starting on 10 March, reflecting increased mixing as interventions and/or behaviour were relaxed following the peak in reported cases. The magnitude and duration of the increase in R_{EI} was scenario-dependent (see Table 1). Immunity in the population from vaccination and from prior infection reduce the effective reproduction number below the assumed value of R_{EI}. This was calculated dynamically within the model as it depends on age-specific, time-varying vaccine coverage, rate of prior infection, and waning. We assumed the generation time distribution (in the absence of quarantine or isolation measures) is a Weibull distribution with mean $\bar{g} = 3.3$ days and s.d. 1.3 days (12).

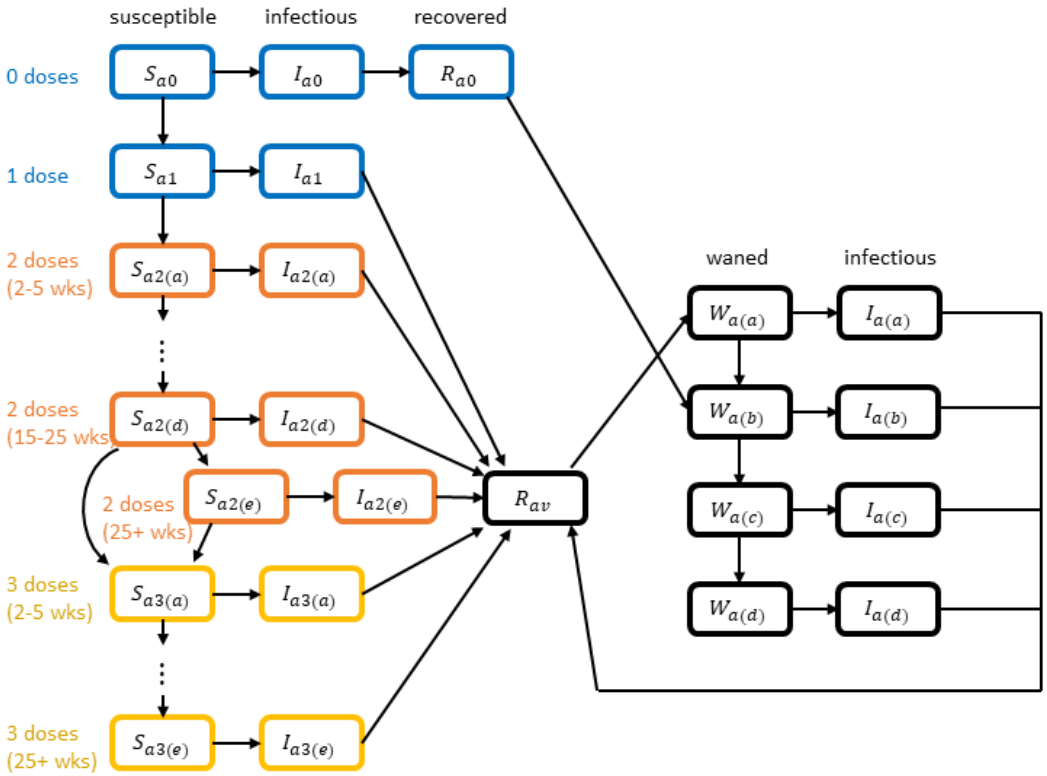

Supplementary Figure S3. Schematic diagram showing how individuals transition between model compartments. Compartments are coloured according to the type of immunity: 0-1 doses and no prior infection (blue); two doses and no prior infection (orange); three doses and no prior infection (yellow); prior infection (black). Transition between different colours occur as a result of receiving a dose of the vaccine or recovering from infection. Transition between susceptible compartments of the same colour occur as a result of waning immunity over time. People whose first infection occurs after they have had at least one dose of the vaccine transition initially into compartment W(a) following recovery; people whose first infection occurs when they are unvaccinated transition initially into compartment W(b) following recovery reflecting lower levels of infection-derived immunity in unvaccinated people; following recovery from second or subsequent infection, people transition initially into compartment W(a) regardless of vaccination status. The model consists of 16 five-year age bands; for simplicity the diagram only shows compartments for one age group a.

Waning of infection-induced immunity

Following infection, individuals were assumed to remain completely immune to re-infection for a fixed period of 30 days. At the end of this period, they moved to the first of a series of four age-specific waned compartments, labelled W(a) (Supplementary Figure S3). To model progressive waning with time since last infection, individuals in waned compartments W(a), W(b) and W(c) transitioned to waned compartment W(b), W(c) and W(d) respectively at constant rate r_w, thus moving through a series of compartments with progressively lower levels of immunity (Supplementary Table S1). Individuals in compartment W(d) remained there until they became infected. Individuals whose first infection occurred when they are unvaccinated transitioned initially into the W(b) compartment following recovery rather than the W(a) compartment. This modelling assumption reflected lower levels of immunity following infection in unvaccinated people than in vaccinated people. Following recovery from a second or subsequent infection, all individuals transitioned initially to W(a), regardless of vaccination status. This set of compartments creates a cycle of infection and waning.

The simplest model of waning of infection-derived immunity would have a single compartment for individuals who are susceptible following recovery from infection, rather than the four compartments used in our model. However, having a single compartment would mean that average immunity following recovery decays exponentially to a specified asymptote. The drop in immunity, whether against infection or severe illness, would always be at its fastest immediately after recovery, which is not necessarily realistic. The use of four post-infection susceptible compartments enabled the model to capture different immunity waning curves for different clinical endpoints.

The immunity curves shown in Figure 1 represent the average immunity of a cohort of individuals who were infected at the same time as they progress through compartments W(a)–W(d). The average immunity $\bar{e}(t)$ at time t after entering compartment W(a) (indexed here by $k = 1$) was calculated as $\bar{e}(t) = \sum_k e_k q_k(t)$ where e_k is the immunity level for compartment k (see Supplementary Table S1) and $q_k(t)$ is the proportion of the cohort in compartment k at time t, which satisfies $q_1(0) = 1$, $q_k(0) = 0$ for $k > 1$, and

$$\frac{dq_k}{dt} = \begin{cases} -r_w q_k & k = 1 \\ r_w(q_{k-1} - q_k) & k = 2, 3 \\ r_w q_{k-1} & k = 4 \end{cases}$$

Values of the immunity parameters in Supplementary Table S1 were chosen such that $\bar{e}(t)$ to approximated the infection-derived immunity estimates of (6) based on the model of (4, 5).

A sensitivity analysis was run in which infection-derived immunity to hospitalisation and death waned more rapidly. In this scenario, the immunity to hospitalisation and death parameters for the final waned compartment W(d) were set to 79%. All other immunity parameters were kept the same as the "fast waning" scenario (Supplementary Table S1). Results of this sensitivity analysis can be found in Supplementary Table S5 and Supplementary Figure S6.

Compartment	Infection	Hospitalisation	Death
S0	0%	0%	0%
S1	0%	0%	0%
S2(a)	62%	83%	92%
S2(b)	55%	80%	90%
S2(c)	40%	75%	87%
S2(d)	28%	72%	86%
S2(e)	5%	63%	82%
S3(a)	64%	92%	96%
S3(b)	57%	88%	94%
S3(c)	47%	83%	92%
S3(d)	40%	79%	90%
S3(e)	10%	69%	85%
baseline			
W(a)	89%	100%	100%
W(b)	80%	100%	100%
W(c)	66%	98%	98%
W(d)	50%	94%	94%
slow waning			
W(a)	93%	100%	100%
W(b)	88%	100%	100%
W(c)	66%	98%	98%
W(d)	10%	89%	89%
fast waning			
W(a)	89%	100%	100%
W(b)	80%	100%	100%
W(c)	55%	98%	97%
W(d)	5%	89%	89%

Supplementary Table S1. Assumed immunity parameters for the model's 16 susceptible compartments. For the "dose 2" and "dose 3" compartments, these parameters correspond to vaccine effectiveness estimates for the Pfizer/BioNTech BNT162b2 vaccine against Omicron (13). For the "waned" compartments, these parameters correspond to decreasing levels of immunity with increasing time since last infection. People whose first infection occurs after they have had at least one dose of the vaccine transition initially into compartment W(a) following recovery; people whose first infection occurs when they are unvaccinated transition initially into compartment W(b) following recovery, reflecting lower levels of infection-derived immunity in unvaccinated people; following recovery from second or subsequent infection, people transition initially into compartment W(a) regardless of vaccination status. For the baseline and fast waning scenario, the transition rate between "waned" compartments is $r_w = 0.0143$ day^{-1}; for the slow waning scenario $r_w = 0.0063$ day^{-1}.

Age-structured transmission model

Transmission between age groups is described by a next generation matrix, whose (i, j) element is defined to be the expected number of secondary infections in age group i caused by an infected individual in age group j given a fully susceptible population:

$$NGM_{ij} = U\left(p_{clin,j} + \tau\left(1 - p_{clin,j}\right)\right) u_i M_{ji} \quad \text{(S1)}$$

where u_i is the relative susceptibility to infection of age group i, M is a contact matrix describing mixing rates between and within age groups, U is a constant representing the intrinsic transmissibility of the virus.

The contact matrix M is based on the results of (3), adjusted for the New Zealand population by (11). To model higher contact rates in younger age groups relative to older groups, consistent with the observed age distribution of cases during the initial part of New Zealand's Omicron wave, we adjusted the contact matrix by applying different multiplicative factors to blocks of the original contact matrix (Supplementary Table S2). This is an arbitrary adjustment to the contact matrix that results in a younger age distribution of cases, comparable with relevant empirical data (see Figure 5, main text). Other adjustments could also be made and the results for the adjusted contact matrix in scenario C.2 (Supplementary Table S2) are intended as a single illustration of the sensitivity of the model to assumptions about age-dependent contact rates.

The reproduction number excluding the effects of immunity, R_{EI}, is equal to the dominant eigenvalue of the next generation matrix, denoted $\rho(NGM)$. For both the baseline and the adjusted contact matrix, the value of U was chosen so that $\rho(NGM)$ is equal to the assumed value of R_{EI} (see Supplementary Table S4).

The number of people in age group j and susceptible compartment k ($k = 1, \ldots 16$) who are infected by clinical individual l between time t and $t + \delta t$ is a Poisson distributed random variable with mean:

$$\lambda_{l,jk}(t) = Y_l F_l(t) \left(\int_t^{t+\delta t} w(t' - t_{inf,l}) dt' \right) NGM^{clin}_{j,a_l} (1 - e_{Ik}) s_{jk}(t) \qquad \text{(S2)}$$

where:

- Y_l is a gamma distributed random variable with mean 1 and variance $1/k$ representing individual heterogeneity in transmission (14). We set $k = 0.5$ which represents a moderate level of over-dispersion consistent with estimates for SARS-CoV-2 transmission patterns (15, 16).
- $F_l(t)$ represents the effect of quarantine or isolation on the transmission rate of individual l at time t, and is equal to 1 if individual l is not in quarantine/isolation at time t, equal to c_{quar} if individual l is in quarantine, and equal to c_{isol} if individual l is in isolation.
- $w(t')$ is the probability density function of the assumed generation time distribution and $t_{inf,l}$ is the time individual l was infected.
- $NGM^{clin}_{j,a_l} = U u_j M_{a_l,j}$ is the next generation matrix for clinical individuals and a_l is the age group of individual l.
- $s_{jk}(t)$ is the fraction of age group j that is in susceptible compartment k at time t.
- e_{Ik} is the immunity against infection for susceptible compartment k (see Supplementary Table S1).

The expression for $\lambda_{l,jk}(t)$ above is multiplied by τ if individual l is subclinical. Note that the factor Y_l means that, in the absence of control measures, the total number of people infected by a randomly selected individual has a negative binomial distribution with mean R_0 and variance $R_0(1 + R_0/k)$ (14).

	Baseline						Scenario C.2 from 1 July 2022 onwards					
Age	0-14	15-24	25-34	35-49	50-59	60+	0-14	15-24	25-34	35-49	50-59	60+
0-14	1.1	0.7	0.55	0.45	0.45	0.5	1.1	0.7	0.6	0.6	0.5	0.6
15-24		1.2	0.7	0.5	0.5	0.3		1.1	0.7	0.6	0.5	0.6
25-34			1.1	0.5	0.5	0.5			1.2	0.6	0.5	0.6
35-49				0.15	0.15	0.45				0.5	0.5	0.6
50-59					0.15	0.45					0.3	0.6
60+						0.15						0.9

Supplementary Table S2. Contact matrix multipliers applied to the original New Zealand contact matrix of (11). All multiplicative factors are applied symmetrically above and below the main diagonal.

Disease severity

The assumed risk of hospitalisation and death in five-year age bands for infections in unvaccinated people is shown in Supplementary Table S3 – see (1) for details of data sources. The assumed infection fatality rate for the over 75 year age group is higher than the value used in (1) by a factor of 1.6 to give a better match with the observed case fatality rate in this group (3.1%).

Clinical individuals in age group i and susceptible compartment k at the time of infection were assumed to require hospitalisation with probability $(1-e_{D,k})/(1-e_{S,k})\,p_{hosp,i}/p_{clin,i}$, where $p_{hosp,i}$ is the infection to hospitalisation ratio for immune naive people in age group i . The time between symptom onset and hospitalisation was assumed to be exponentially distributed with mean 5 days (this assumption affects the timing but not the number of hospital admissions). The length of hospital stay is assumed to be exponentially distributed with mean $t_{LOS} = 4$ days (17). Hospitalised cases in age group i die with probability $(1-e_{M,k})/(1-e_{D,k})\,IF\,R_i/p_{hosp,i}$ where IFR_i is the infection fatality ratio for immune naive cases in age group i. For simplicity, the date of death is assumed to be the same as the date of hospital discharge. In reality, the average time from hospital admission to death is longer (this simplifying assumption means that deaths will be more lagged relative to cases in reality than in the model but does not affect the total number of deaths).

Age band (years)															
0-4	5-9	10-14	15-19	20-24	25-29	30-34	35-39	40-44	45-49	50-54	55-59	60-64	65-69	70-74	75+
Proportion of infections causing hospitalisation (%)															
0.31	0.31	0.13	0.20	0.29	0.42	0.61	0.90	1.27	1.87	2.77	3.90	5.65	7.94	11.1	19.9
Proportion of infections causing death (%)															
0.0004	0.0004	0.0004	0.0008	0.002	0.003	0.006	0.011	0.023	0.045	0.087	0.168	0.331	0.635	1.22	6.83

Supplementary Table S3. Hospitalisation and death rates for unvaccinated infected people in five-year age bands. Rates are the same is in (1), based on (18, 19), except for the fatality rate in the over 75 year age group which was increased by a factor of 1.6 to provide a better match with New Zealand's observed case fatality rate in this age group.

Parameter	Value
Initial reproduction number excluding effects of immunity	$R_{EI} = 2.5$
Incubation period	Mean 3.6 days, s.d. 1.5 days
Generation interval	Mean 3.3 days, s.d. 1.3 days
Relative infectiousness of subclinical individuals	$\tau = 0.5$
Heterogeneity in individual reproduction number	$k = 0.5$
Probability of detection for clinical individuals (up to 22 Feb 2022)	$p_{test} = 0.3$
Probability of detection for clinical individuals (from 23 Feb 2022)	$p_{test} = 0.5$
Probability of a contact of a confirmed case being traced	$p_{trace} = 0.25$
Relative transmission rate for individuals in quarantine	$c_{quar} = 0.5$
Relative transmission rate for individuals in isolation (up to 22 Feb 2022)	$c_{isol} = 0.2$
Relative transmission rate for individuals in isolation (from 23 Feb 2022)	$c_{isol} = 0.5$
Time from symptom onset to test result (up to 22 Feb 2022)	Mean 4.0 days, s.d. 4.0 days
Time from symptom onset to test result (from 23 Feb 2022)	Mean 1.5 days, s.d. 1.5 days
Time from confirmation of case to quarantine of contacts	Mean 3.0 days, s.d. 1.7 days
Time form symptom onset to hospital admission	Mean 5.0 days, s.d. 5.0 days
Length of hospital stay	Mean 4.0 days, s.d. 4.0 days

Age-specific parameters																
Age (yrs)	0-4	5-9	10-14	15-19	20-24	25-29	30-34	35-39	40-44	45-49	50-54	55-59	60-64	65-69	70-74	75+
Pr(clinical) (%)	54.4	55.5	57.7	59.9	62.0	64.0	65.9	67.7	69.5	71.2	72.7	74.2	75.5	76.8	78.0	80.1
Susceptibility*	0.46	0.46	0.45	0.56	0.79	0.93	0.97	0.98	0.94	0.93	0.94	0.97	1.00	0.98	0.90	0.86
Popn (1000s)	305	328	337	317	330	370	379	341	312	325	333	326	299	255	220	346

Supplementary Table S4. Other parameter values used in the model. *Susceptibility for age group i is stated relative to susceptibility for age 60-64 years.

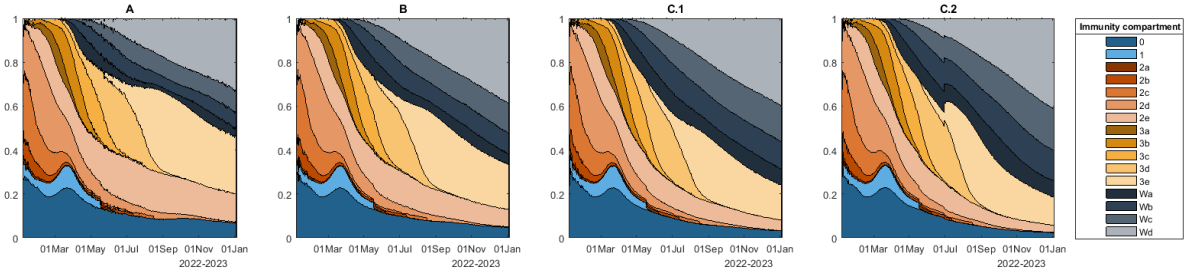

Supplementary Figure S4. Proportion of daily reported cases that were infected from each of the 16 susceptible compartments at the time of infection for the four baseline scenarios A, B, C.1 and C.2. Blue, red and yellow shades represent people infected for the first time who have had 0/1 doses, 2 doses or 3 doses of the vaccine respectively. Grey shades represent people being infected for the second or subsequent time. Re-infections are small part of the first wave up to May 2022, but account for a steadily increasing fraction of all cases from June 2022 onwards.

Scenario	Infections	Cases	Hospitalisations	Deaths
A	4,764,000	1,798,000	25,700	1,490
B	6,308,000	2,406,000	34,900	2,220
C.1	7,416,000	2,845,000	41,800	2,860

Supplementary Table S5. Total number of infections, cases, hospitalisations and deaths in the model over the simulated time period (365 days starting on 5 January 2022) under the sensitivity analysis in which infection-derived immunity to hospitalisation and death waned more rapidly (immunity to hospitalisation and death for compartment W(d) set to 79%, all other immunity parameters as in the "fast waning" scenario in Supplementary Table S1).

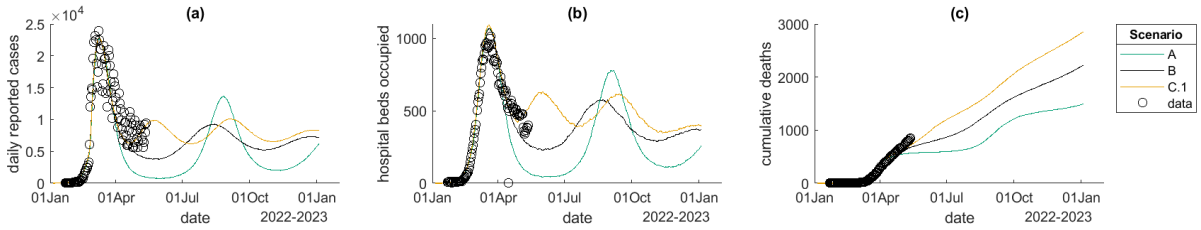

Supplementary Figure S5. Model results for daily reported cases (a), number of hospital beds occupied (b), and cumulative deaths (c) for the three scenarios A (green), B (black) and C.1 (solid yellow), under the sensitivity analysis in which infection-derived immunity to hospitalisation and death waned more rapidly (immunity to hospitalisation and death for compartment W(d) set to 79%, all other immunity parameters as in the "fast waning" scenario in Supplementary Table S1). Black circles show data up to 12 May 2022.

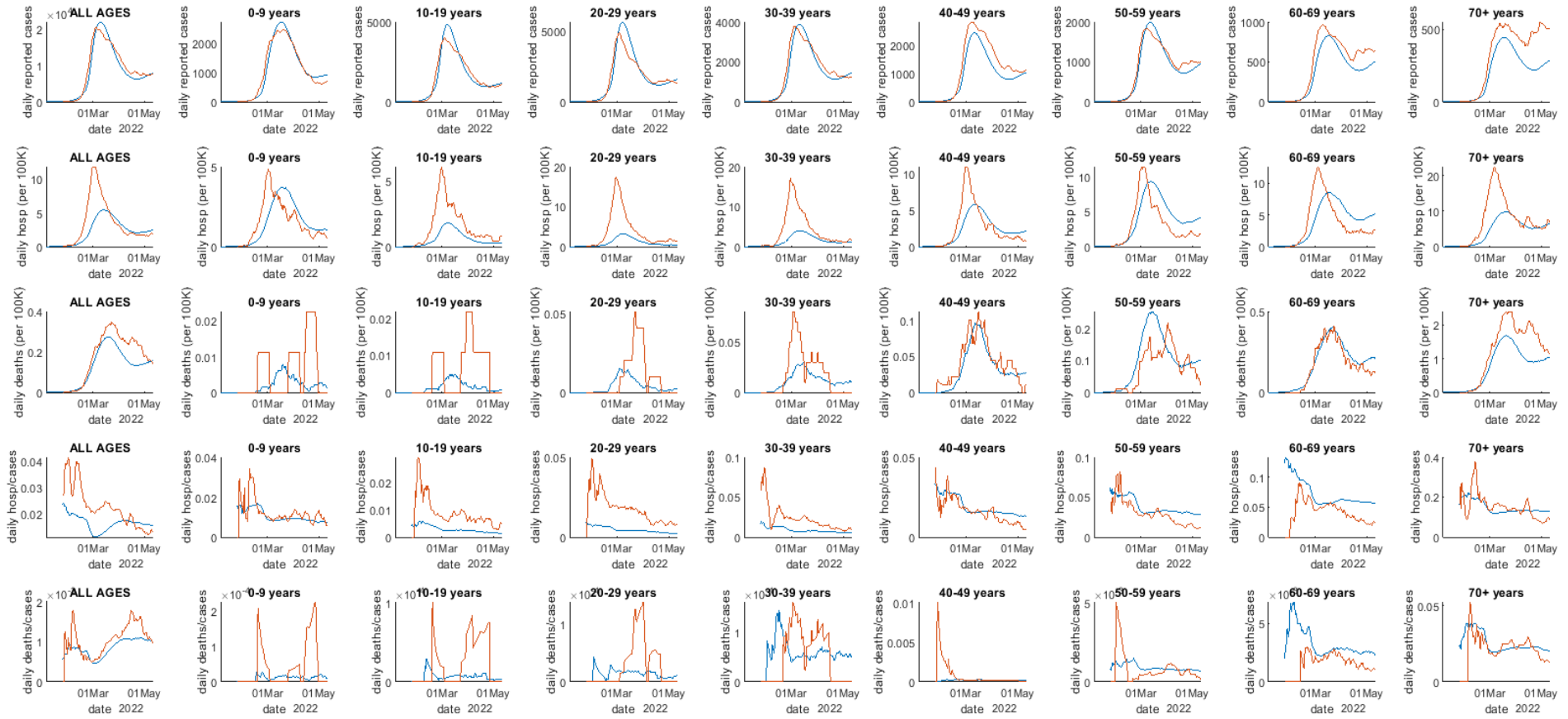

Supplementary Figure S6. Comparison of daily reported cases, daily hospitalisations per 100,000 population, daily deaths per 100,000 population, hospitalisation:case ratio, and death:case ratio stratified by ten-year age bands, for baseline model scenario C.1 (blue curves) with data up to 12 May 2022 (red curves). The hospitalisations data is for the Northern region (Auckland, Counties Manukau, Waitematā and Northland District Health Boards). Note different y-axis scales for different age bands.

References

1. Vattiato G, Maclaren O, Lustig A, Binny RN, Hendy SC, Plank MJ. An assessment of the potential impact of the Omicron variant of SARS-CoV-2 in Aotearoa New Zealand. Infectious Disease Modelling. 2022;7:94-105.
2. Anderson RM, May RM. Infectious Diseases of Humans: Dynamics and Control: OUP Oxford; 1992.
3. Prem K, Cook AR, Jit M. Projecting social contact matrices in 152 countries using contact surveys and demographic data. PLoS Computational Biology. 2017;13(9):e1005697.
4. Khoury DS, Cromer D, Reynaldi A, Schlub TE, Wheatley AK, Juno JA, et al. Neutralizing antibody levels are highly predictive of immune protection from symptomatic SARS-CoV-2 infection. Nature Medicine. 2021;27(7):1205-11.
5. Cromer D, Steain M, Reynaldi A, Schlub TE, Wheatley AK, Juno JA, et al. Neutralising antibody titres as predictors of protection against SARS-CoV-2 variants and the impact of boosting: a meta-analysis. The Lancet Microbe. 2022;3(1):e52-e61.
6. Golding N, Lydeamore M. Analyses to predict the efficacy and waning of vaccines and previous infection against transmission and clinical outcomes of SARS-CoV-2 variants 2022. Available from: https://github.com/goldingn/neuts2efficacy.
7. Steyn N, Binny RN, Hannah K, Hendy S, James A, Lustig A, et al. Māori and Pacific People in New Zealand have higher risk of hospitalisation for COVID-19. New Zealand Medical Journal. 2021;134(1538):28-43.
8. Golding N, Price DJ, Ryan GE, McVernon J, McCaw JM, Shearer FM. Estimating the transmissibility of SARS-CoV-2 during periods of high, low and zero case incidence. medRxiv. 2021:2021.11.28.21264509.
9. Chen C, Nadeau S, Yared M, Voinov P, Xie N, Roemer C, et al. CoV-Spectrum: analysis of globally shared SARS-CoV-2 data to identify and characterize new variants. Bioinformatics. 2021;38(6):1735-7.
10. Khan K, Karim F, Ganga Y, Bernstein M, Jule Z, Reedoy K, et al. Omicron sub-lineages BA.4/BA.5 escape BA.1 infection elicited neutralizing immunity. medRxiv. 2022:2022.04.29.22274477.
11. Steyn N, Plank MJ, Binny RN, Hendy S, Lustig A, Ridings K. A COVID-19 vaccination model for Aotearoa New Zealand. Scientific Reports. 2022;12:2720.
12. Abbott S, Sherratt K, Gerstung M, Funk S. Estimation of the test to test distribution as a proxy for generation interval distribution for the Omicron variant in England. medRxiv. 2022: https://doi.org/10.1101/2022.01.08.22268920.
13. Andrews N, Stowe J, Kirsebom F, Toffa S, Rickeard T, Gallagher E, et al. Covid-19 Vaccine Effectiveness against the Omicron (B.1.1.529) Variant. New England Journal of Medicine. 2022:10.1056/NEJMoa2119451.
14. Lloyd-Smith JO, Schreiber SJ, Kopp PE, Getz WM. Superspreading and the effect of individual variation on disease emergence. Nature. 2005;438(7066):355-9.
15. James A, Plank MJ, Hendy S, Binny RN, Lustig A, Steyn N. Model-free estimation of COVID-19 transmission dynamics from a complete outbreak. PLoS ONE. 2020;16:e0238800.
16. Riou J, Althaus CL. Pattern of early human-to-human transmission of Wuhan 2019 novel coronavirus (2019-nCoV), December 2019 to January 2020. Eurosurveillance. 2020;25(4):2000058.

17. Abdullah F, Myers J, Basu D, Tintinger G, Ueckermann V, Mathebula M, et al. Decreased severity of disease during the first global Omicron variant Covid-19 outbreak in a large hospital in Tshwane, South Africa. International Journal of Infectious Diseases. 2021: https://doi.org/10.1016/j.ijid.2021.12.357.
18. Herrera-Esposito D, de los Campos G. Age-specific rate of severe and critical SARS-CoV-2 infections estimated with multi-country seroprevalence studies. BMC Infectious Diseases. 2022;22:311.
19. Nyberg T, Ferguson NM, Nash SG, Webster HH, Flaxman S, Andrews N, et al. Comparative analysis of the risks of hospitalisation and death associated with SARS-CoV-2 omicron (B.1.1.529) and delta (B.1.617.2) variants in England: a cohort study. Lancet. 2022;399(10332):1303-12.